OCCUPANT MOTION SENSORS:
DEVELOPMENT AND TESTING OF A PIEZORESISTIVE MOUTHPIECE ROTATIONAL ACCELEROMETER

G. Plank
D. Ofsevit
A. Warner

JULY 1973

INTERIM REPORT

Prepared for

DEPARTMENT OF TRANSPORTATION
NATIONAL HIGHWAY TRAFFIC SAFETY ADMINISTRATION
Research Institute
Washington DC 20590

1. Report No.	2. Government Accession No.	3. Recipient's Catalog No.

4. Title and Subtitle	5. Report Date
OCCUPANT MOTION SENSORS: DEVELOPMENT AND TESTING OF A PIEZORESISTIVE MOUTHPIECE ROTA-TIONAL ACCELEROMETER	July 1973
	6. Performing Organization Code

7. Author(s)	8. Performing Organization Report No.
G. Plank, D. Ofsevit, A. Warner	DOT-TSC-NHTSA-73-5

9. Performing Organization Name and Address	10. Work Unit No. (TRAIS)
Transportation Systems Center Kendall Square Cambridge, MA 02142	R3406/HS305
	11. Contract or Grant No.
	13. Type of Report and Period Covered

12. Sponsoring Agency Name and Address	
Department of Transportation National Highway Traffic Safety Administration Research Institute Washington, DC 20590	Interim Report
	14. Sponsoring Agency Code

15. Supplementary Notes

16. Abstract

    A miniature piezoresistive mouthpiece rotational accelerometer has been developed to measure the angular acceleration of a head during a simulated vehicle crash. Corrections have been electronically applied to the rotational accelerometer to reduce its linear sensitivity. The device has been successfully tested in the laboratory on a high speed shake table and in the field using humans and dummies. ues New Techniques in photogrammetry have been developed to speed the reduction of motion picture data.

17. Key Words Occupant Motion, Crash Tests, Rotational Accelerometer, Piezoresistive, Data Reduction, Photogrammetry, High-Speed Film.	18. Distribution Statement DOCUMENT IS AVAILABLE TO THE PUBLIC THROUGH THE NATIONAL TECHNICAL INFORMATION SERVICE, SPRINGFIELD, VIRGINIA 22151.		
19. Security Classif. (of this report) Unclassified	20. Security Classif. (of this page) Unclassified	21. No. of Pages 42	22. Price

Form DOT F 1700.7 (8-72)   Reproduction of completed page authorized

PREFACE

The work described in this report was performed as a part of the Occupant Motion Sensors Program, sponsored by the National Highway Traffic Safety Administration. The objective of this program is to develop effective means of acquiring occupant positional data during a simulated crash. A significant effort has been directed toward the development of a device to measure head rotational acceleration and a rotational accelerometer has been built and tested in the field. The accelerometer is described and the field test results are presented in this report.

Much of the work described in this report has been done with the assistance of personnel at the Daisy Decelerator at Holloman Air Force Base in New Mexico. We wish to thank Major H. Russell of Holloman AFB for his cooperation in this effort.

CONTENTS

LIST OF ILLUSTRATIONS

1. INTRODUCTION

1.1 OBJECTIVE

The objective of the Occupant Motion Sensor Program at TSC
is to develop practical instrumentation to accurately measure
human, animal or dummy motions during a simulated vehicle crash.
Since rapid deceleration of the head can cause brain injury, head
acceleration is usually monitored during restraint systems test-
ing. Off-the-shelf linear accelerometers are commonly used to
measure the linear acceleration. The other component of head
acceleration, rotational acceleration, however, is much more
difficult to measure and is not always measured by field crash
investigators. For this reason TSC is developing a miniature
mouthpiece rotational accelerometer. This report describes this
accelerometer and data obtained with it.

1.2 BACKGROUND

During FY71 an analysis and trade-off study was performed,
a list of five promising systems for obtaining body kinematic
measurements was developed and prototype systems were built and
evaluated.* During FY72 a major effort was directed to the fur-
ther development of one of the five systems: the mouthpiece
rotational accelerometer. The effort was concentrated on the
development of this device because the need for a rotational
accelerometer is great and fabrication of the device appeared to
be possible using readily available components.

The rotational accelerometer consists of two linear accelero-
meters with parallel sensitive axes separated by a known distance.*
The outputs are summed to produce rotational information. The
first developmental device (Figure 1) utilized piezoelectric accele-
rometers which are small, light weight, rugged and have good high
frequency response. As the name implies, a piezoelectric accelero-
meter utilizes the piezoelectric effect. When a piezoelectric

---

*See DOT-TSC-NHTSA-71-4

material such as quartz is subjected to a mechanical stress or deformation it generates an electric charge. In an accelerometer, the piezoelectric material is used to support a seismic mass. Under an acceleration, the mass causes the support to distort, thus producing a charge. The charge, which is proportional to the acceleration, is then processed by signal conditioning electronics and recorded.

Figure 1. Single Axis Piezoelectric Rotational Accelerometer

During field testing of the piezoelectric device in FY72 two problems came to light. The first problem, which is common to all accelerometers, arises from the unit's cross axis sensitivity. The effect is that the rotational accelerometer responds to linear accelerations. The problem was solved by using a linear triaxial accelerometer to correct the rotational output.* The second problem arose during the airbag restraint test at Holloman AFB. When the airbag was not deployed, the piezoelectric accelerometer functioned well with little noise in the signal. However, when the airbag was deployed, the accelerometer signals

---

*DOT-HS-820-211

were obliterated by noise. The exact cause of the noise is still unknown but, as the airbag was expanding, there was a sudden shift in dc signal level. The amplifiers became saturated and did not recover in time to gather valid data. In discussing this with personnel at Holloman, it was thought that a likely cause might be static charge on and around the bag as it was expanding. This would explain the instrumentation noise, as the piezoelectric accelerometers are charge-sensitive devices with a very high output impedance. To solve the problem, it was decided to design a rotational accelerometer that did not utilize piezoelectric devices but used instead piezoresistive devices, which are low impedance devices and less sensitive to static charge. This accelerometer system was much more successful and is the subject of this report.

2. INSTRUMENTATION

2.1 GENERAL

During the latter part of FY72, a piezoresistive rotational accelerometer was used in tests at Holloman Air Force Base in New Mexico. The device consisted of four linear accelerometers arranged in such a fashion that one could measure three orthogonal linear head accelerations as well as rotational acceleration in the sagittal plane. An accompanying electronics package was also built in order to deliver power to the accelerometers, and condition and process the information from each accelerometer. A block diagram of the instrumentation is shown in Figure 2.

2.2 PIEZORESISTIVE ROTATIONAL ACCELEROMETER

The accelerometers chosen for the construction of a piezoresistive rotational accelerometer were Endevco model # 2264-150. Four of these were used and mounted on an aluminum plate that would fit into a mouthpiece. The arrangement was such that one could measure three orthogonal linear accelerations and one rotational acceleration in the sagittal plane. The accelerometer configuration is shown in Figure 3. Each accelerometer incorporates two legs of a dc bridge circuit. When the unit is subjected to an acceleration, the resistance in the two legs changes and causes the bridge to become imbalanced. This arrangement requires a power supply and each accelerometer has two wires for the power supply and two signal wires. The wires from all four accelerometers are incorporated into one cable about 1/8" in diameter. The entire package was coated with epoxy and is shown in Figure 4.

2.3 ELECTRONICS

The electronics consist essentially of a series of bridge completion circuits, conditioning and analog processing circuits and a power supply. For reasons of convenience and safety, it was decided to use batteries for the power supply. Four batteries (Eveready #286 mercury - 8.4 volts), arranged to produce 16.8
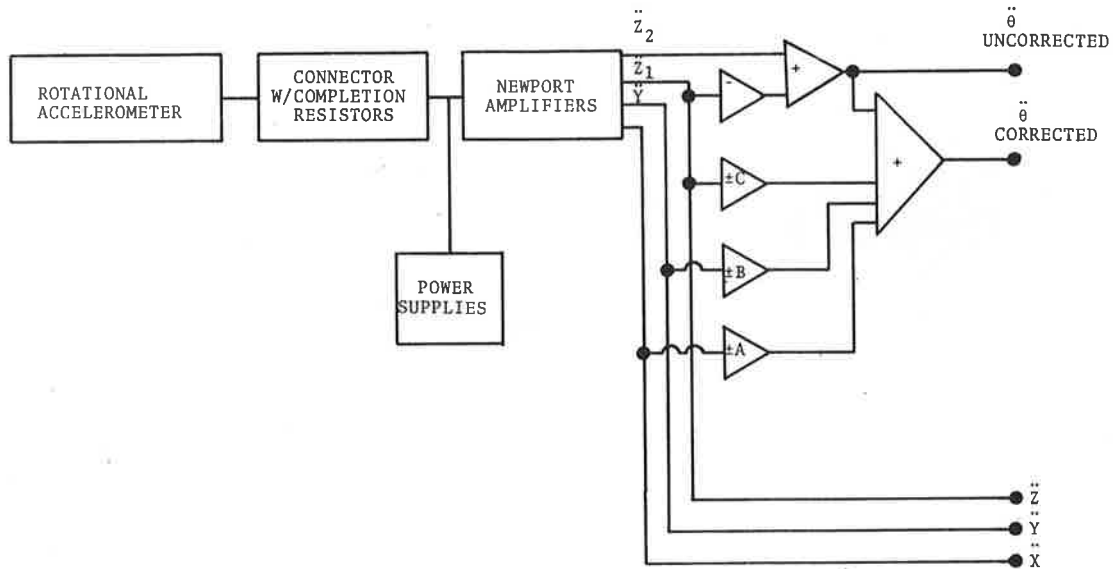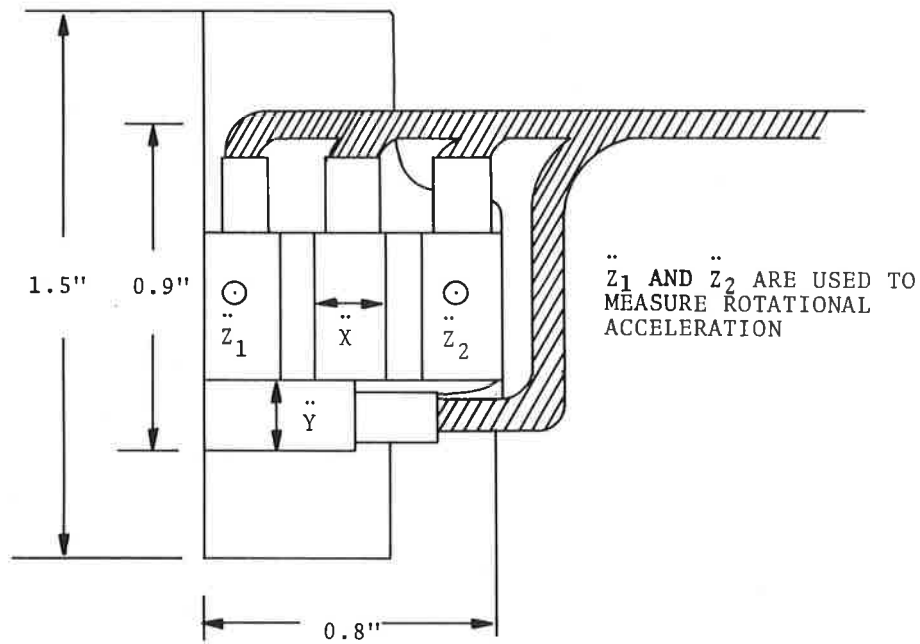
4

Figure 2. Block Diagram of Electronics

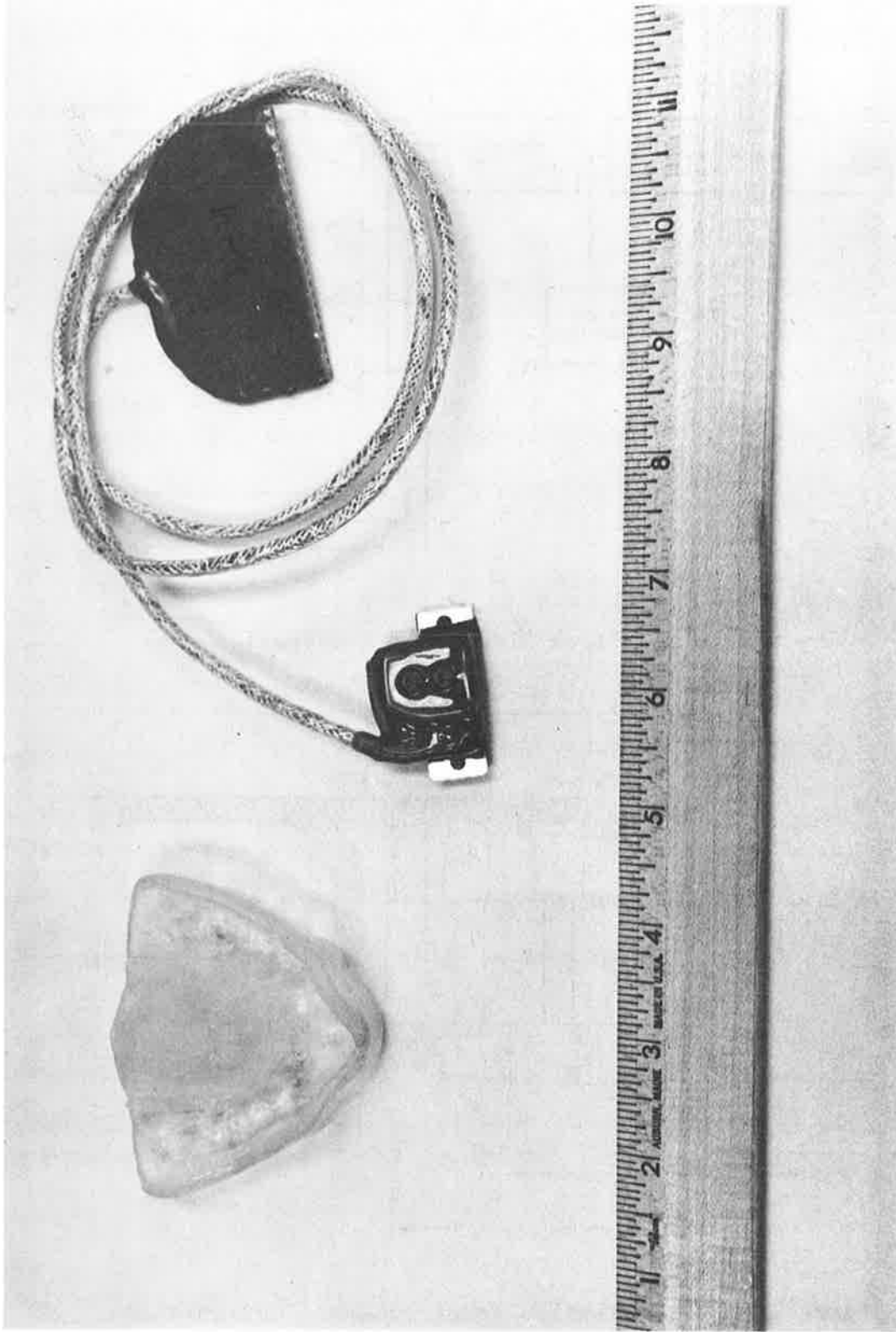Figure 3. Piezoresistive Accelerometer Configuration

Figure 4. Piezoresistive Mouthpiece Accelerometer

volts, are used in conjunction with a Fairchild #723 voltage re-
gulator with the output set at 10 volts. The battery voltage can
drop to 13 volts without affecting the output of the regulator
which will remain at 10 volts and maintain its regulation specifi-
cations. With a 10 volt power supply, the sensitivity of each
individual accelerometer was somewhere between 2.0 mv/g and 3.0
mv/g. The sensitive of each accelerometer was adjusted to
2.0 mv/g with a potentiometer in series with the power supply.
Included also was a zero adjustment for nulling the output with
zero input. A switchable calibration signal is incorporated in-
to the bridge circuit by shunting one leg of the bridge by a
resistor. The circuit arrangement is shown in Figure 5 and the
sensitivity adjustment, zero adjustment and calibration switches
can be seen on the front panel of the main electronics package
in Figure 6. The bridges are completed at the accelerometer
connector and the signal is brought from the sled to the main
electronics package through an umbilical cable. The connector
can be seen in Figure 4 and an X-ray of the connector with its
completion resistors is shown in Figure 7. Knots are tied in the
wires within the connector before potting to provide a strain
relief. The signals first go to a differential amplifier (Newport
model 70-4). From the differential amplifier, a single ended
signal goes to a group of operational amplifiers where analog
processing takes place.

The output of the rotational accelerometer due to linear
accelerations can be reduced by analog processing. The components
which are in phase or 180° out of phase with the rotational output
were eliminated using operational amplifiers. These operational
amplifiers are labeled A, B and C in Figure 2. The amplifiers
employed for this purpose are Philbrick #1021. The residual
linear error is on the order of 3 rad/sec^2/g. After the Newport
amplifiers, the signals are fed to the operational amplifiers for
processing. There are five output terminals which are for the
three orthoganal linear accelerations $\ddot{X}$, $\ddot{Y}$, $\ddot{Z}$, uncorrected rota-
tional acceleration, and corrected rotational acceleration. The
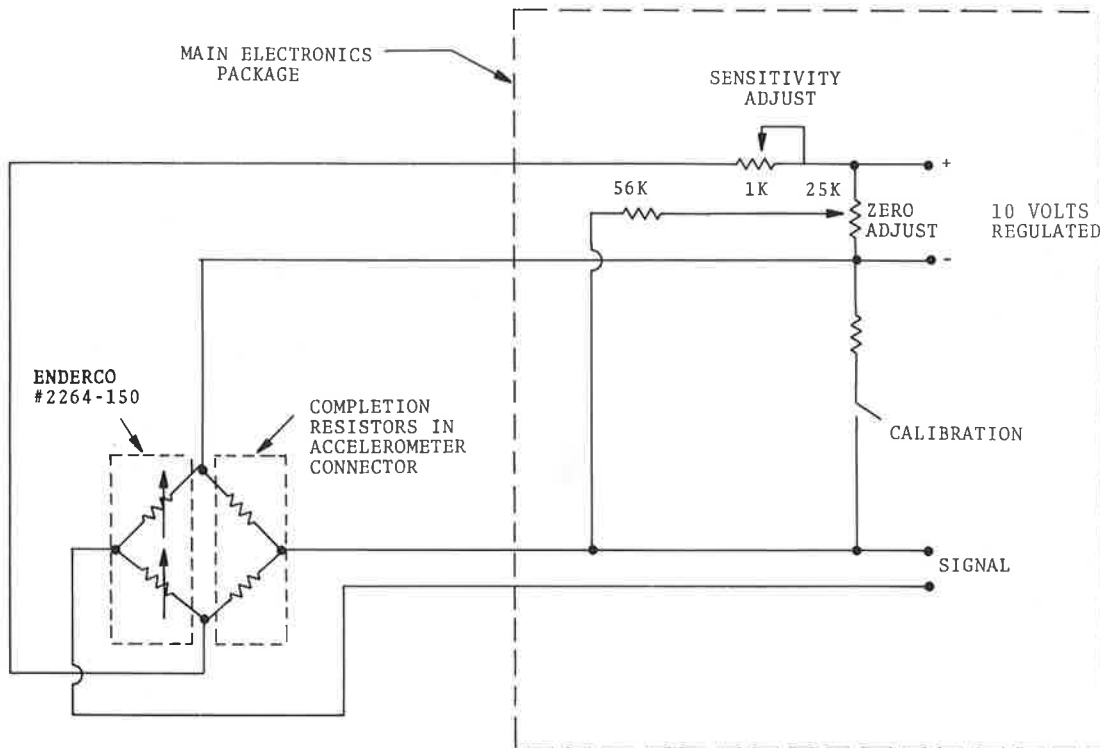signs and coefficients (A, B and C) of the linear error corrections

7

Figure 5. Accelerometer Circuit Arrangement
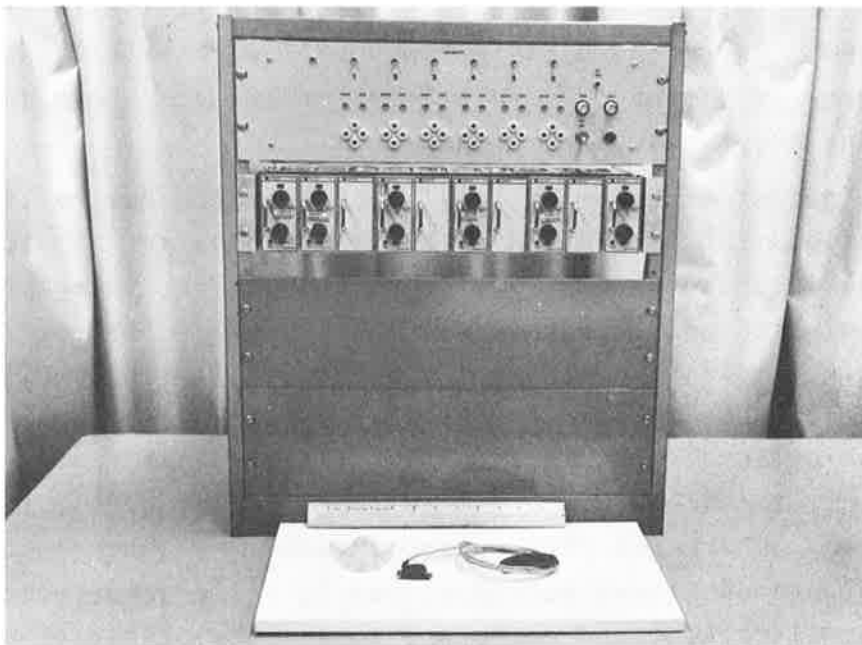
Figure 6. Main Electronics Package

8
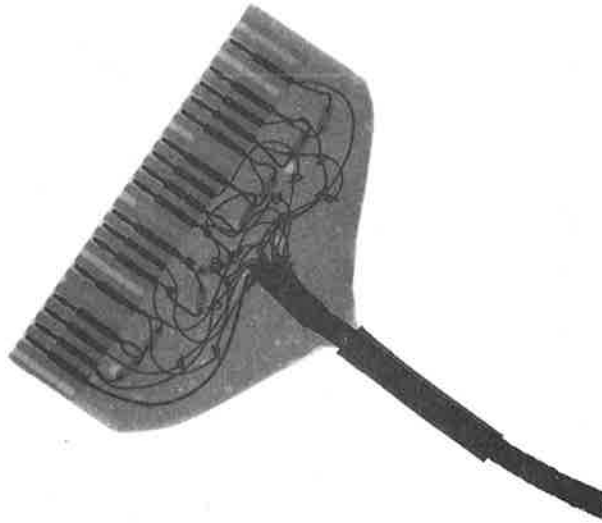
Figure 7. X-Ray of Accelerometer Connector

are adjusted during calibration.

2.4 CALIBRATION

One can determine the corrections necessary by vibrating the accelerometer package in various rotational and linear modes.* The errors can be nulled out while the unit is vibrating.

For the particular accelerometer in question, the errors induced by $\ddot{X}$ and $\ddot{Z}$ proved to be insignificant and the only necessary correction to be made was due to $\ddot{Y}$. Figure 8 shows the error induced by each of the three orthogonal linear accelerations. The accelerometer package was vibrated in each linear mode and the uncorrected rotational output was measured. The output is an error voltage that represents an error in the measurement of rotational acceleration ($\ddot{\theta}$). The errors due to $\ddot{X}$ and $\ddot{Z}$ were very low and were not corrected. They were also equal in magnitude as can be seen in Figure 8. The error due to $\ddot{Y}$ was relatively large and was corrected with analog processing. The

*DOT-HS-820-211

Figure 8. Accelerometer Error Characteristics

Figure 9. Accelerometer Sensitivity

10

magnitude of the corrected output is substantially lower than the magnitude of the uncorrected output, as can be seen in Figure 8. The rotational sensitivity of this accelerometer was .003 mili-volts/r/sec.^{2} and its excellent linearity is apparent in Figure 9.
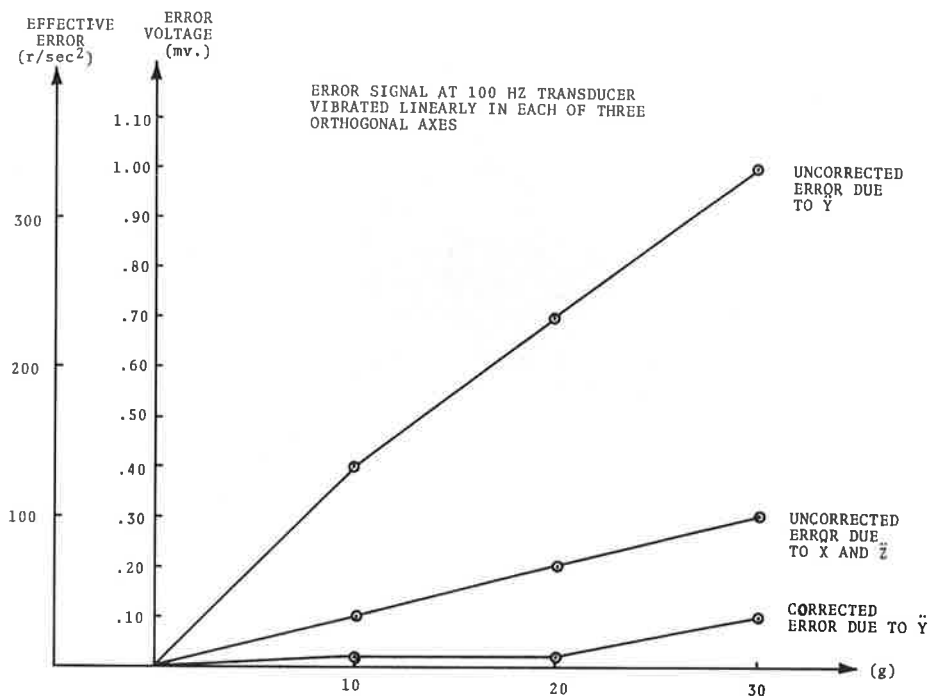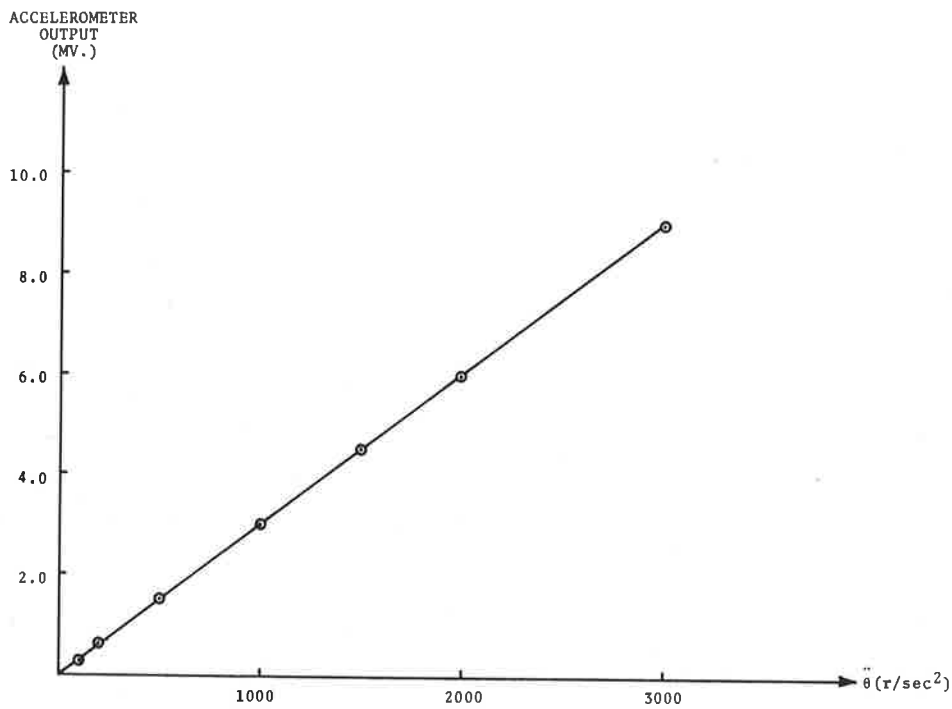
3. FIELD TESTS

3.1 GENERAL

Field tests were made with the previously described piezo-
resistive rotational accelerometer at the Daisy track facility
at Holloman Air Force Base in New Mexico. The tests were made
with humans or dummies seated in a deceleration sled which was
equipped with an airbag (a passive restraint inflatable bag to
prevent occupant impact with the dashboard during a crash).

3.2 OBJECTIVES

The objectives of the tests were to measure the rotational
and linear accelerations of a subject's head in conjunction with
the deployment of an airbag during a simulated crash and to correlate
this information with the information obtained from high speed
films.

3.3 HOLLOMAN TEST CONFIGURATION

The Holloman test configuration consisted of a semi-enclosed
sled with a simulated automobile dashboard and is shown in Figure
10. This illustration is one frame of a high speed film during
an actual test. High speed cameras were employed beside the
track and on the sled. The sled is slowly accelerated on the
track to some predetermined velocity and allowed to coast freely
into a water brake. The water brake is designed to control the
velocity profile of the braking action. The subject was equipped
with lap and shoulder belts in the event that the airbag did not
deploy. Upon impact with the water brake, the bag would inflate
and the safety belts would be released to allow the subject to
move freely into the airbag. If the airbag did not inflate, the
safety belts would not be released.

The rotational accelerometer was mounted on a mouthpiece in
the subject's mouth and the cable was brought out the side of the
mouth to connectors on the sled. The information was then fed

12
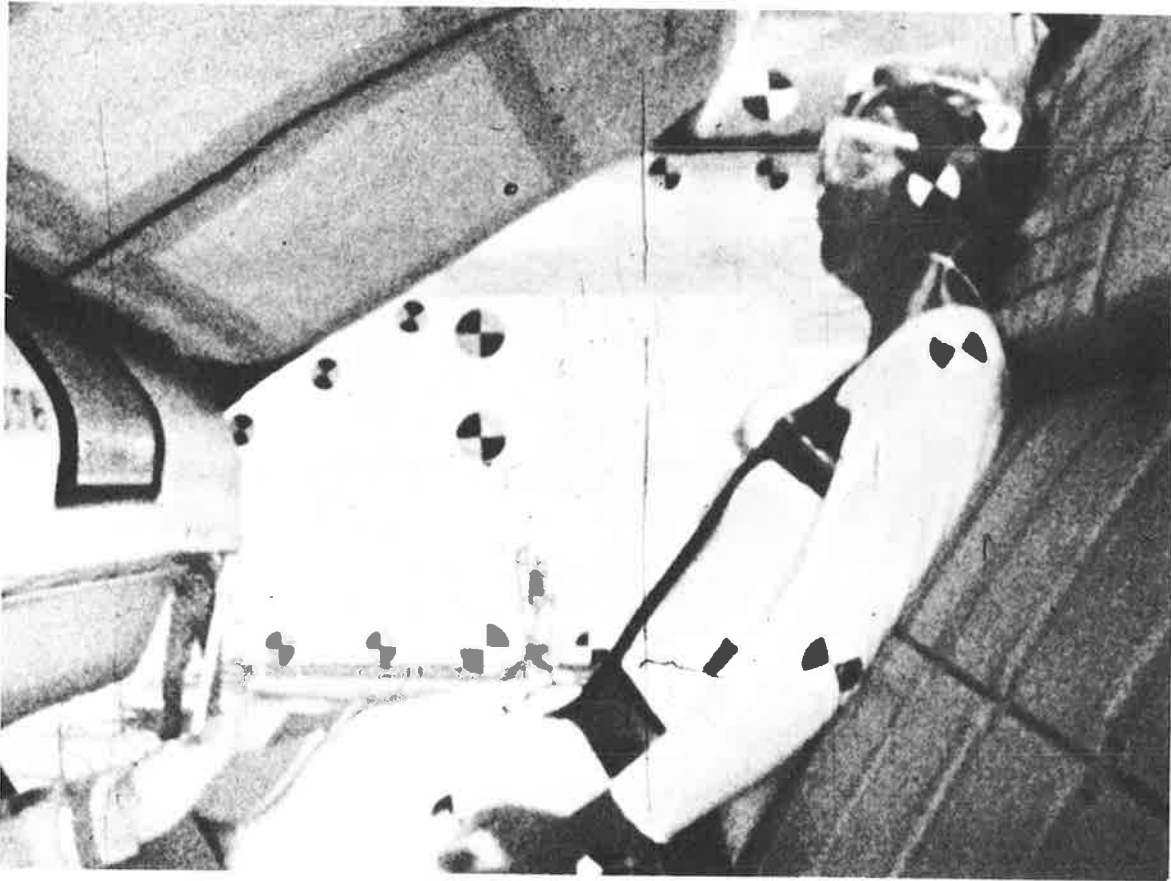
Figure 10. Frame from High Speed Film Showing Interior of Sled

through a long umbilical cable to the instrumentation building. The information that was recorded on magnetic tape during the tests included the three orthogonal linear head accelerations, the sagittal rotational acceleration, sled acceleration, and a voice channel.

3.4 RESULTS

Several tests with the mouthpiece rotational accelerometer were made on humans. The information presented here is considered to be representative of all the tests made.

The information recorded from a typical test is shown in Figure 11. The polarity of the recorded information is illustrated in Figure 12. As can be seen in Figure 11, the peak sled accel-
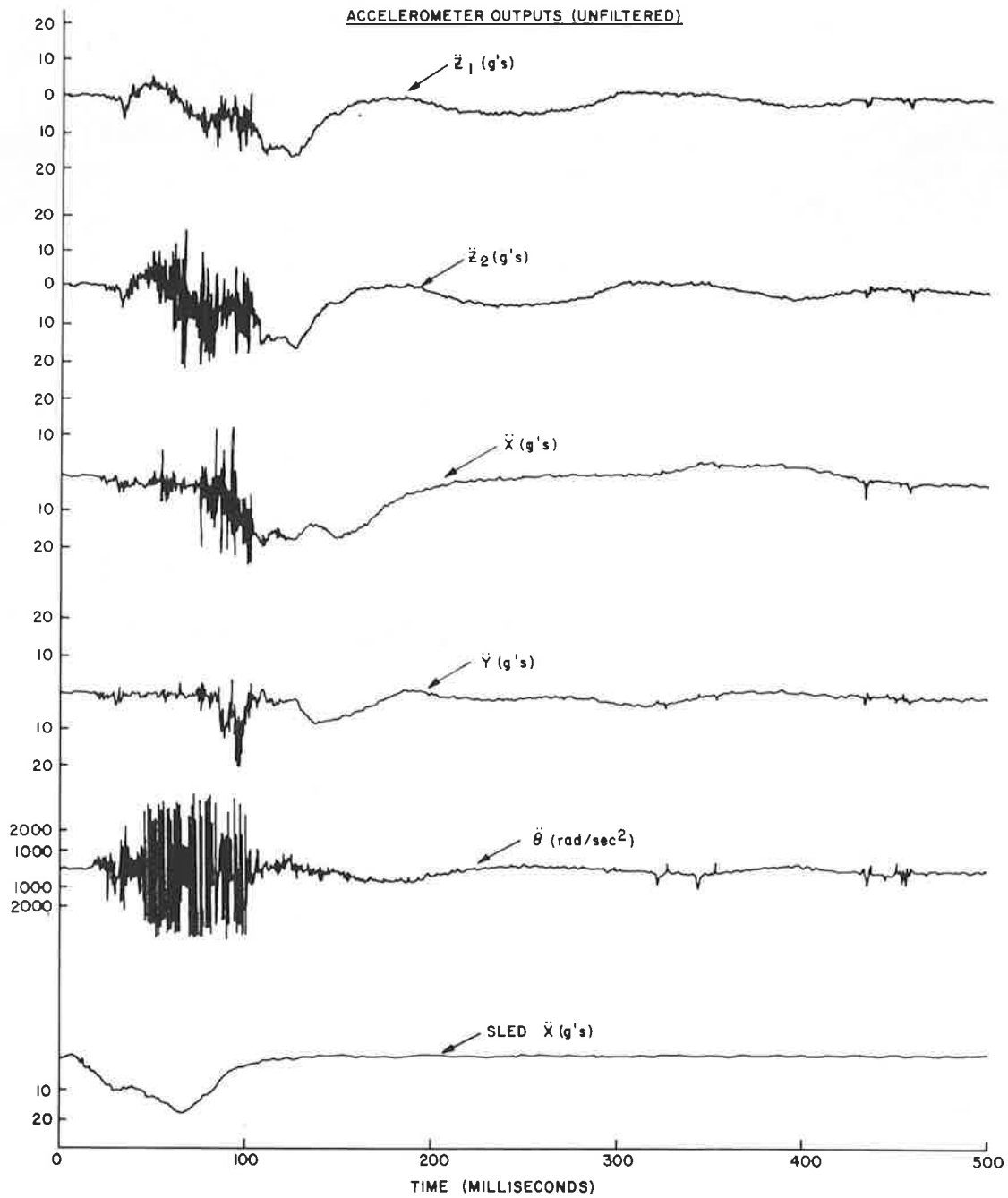
Figure 11. Data From Typical Test

14

eration was slightly under 20 g's. The noise seen initially in each of the data channels occurred while the airbag was expanding and ceased when the bag was fully expanded. As is apparent in the figure, the dominant linear acceleration of the head occurred in the X direction and was close to 20 g's. This was anticipated, as this is the direction of sled deceleration. A slightly smaller level is seen on the two Z accelerometers. These are the two accelerometers that are used to determine rotational acceleration in the sagittal plane. Also, as expected, the acceleration in the Y direction was less than any other linear acceleration. The rotational acceleration measured in the test shown in Figure 11 was about 500 r/sec.^{2}. A more detailed analysis and correlation with film data is given in Sections 4 and 5.

There was little complaint from the subjects about the size or shape of the accelerometer and no noticeable drift due to temperature changes when the accelerometer was placed in the subject's mouth. While there was electrical noise in the signals during the expansion of the airbag, it did not pose the problem that was seen with the piezoelectric devices as the noise level was lower and the amplifiers did not remain in saturation.
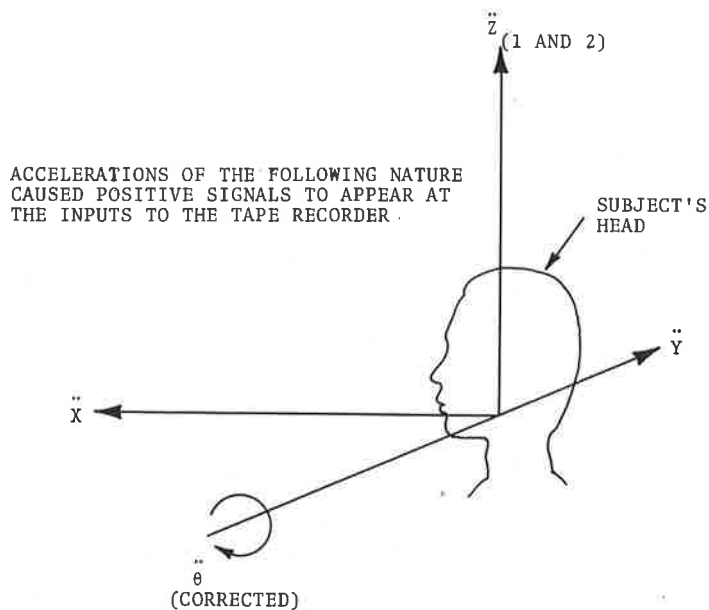

ACCELERATIONS OF THE FOLLOWING NATURE CAUSED POSITIVE SIGNALS TO APPEAR AT THE INPUTS TO THE TAPE RECORDER

$\ddot{Z}$ (1 AND 2)

SUBJECT'S HEAD

$\ddot{Y}$

$\ddot{X}$

$\ddot{\theta}$ (CORRECTED)

Figure 12. Polarity of Recorded Signals

15

4. PHOTOGRAMMETRY

4.1 GENERAL

The principal tool used in motion studies in the past has been the high speed camera. A major problem in this technique has been the extraction of information from the films. Pattern recognition techniques using a computer are very costly and purely manual techniques are extremely tedious. A semi-automated technique has been developed which allows one to gather information on angular position with relative ease.

4.2 BACKGROUND

The high speed motion pictures taken at the deceleration sled test site provide the means for direct measurement of the angular position, θ, of the subject's head.

Since the cameras take approximately 1000 frames per second and a typical crash test contains about 0.5 seconds of meaningful action, some 500 frames must be analyzed for each film of interest. As we shall see, more than one film must sometimes be read in order to obtain a complete graph of θ, as a function of time, for a single crash test.

For analysis, the film is projected frame by frame with a stop-action projector. With the first film reader used in this project, the film was projected onto a drafting table which was tilted to a nearly vertical position. A special cursor, which could be aligned with θ, was attached to one arm of the drafting head mounted on the table. Attached to the cursor was a rotary potentiometer which served as a transducer to convert the position of the cursor to a voltage proportional to θ. For each frame, the operator set the cursor to the target on the projected film image. The output of the rotary potentiometer appeared on a digital voltmeter and the operator recorded this reading by pushing a button on the voltmeter to activate a small printer attached to the voltmeter. Another push-button was used to advance the film

16

to the next desired frame. At the end of the film, the printer
output was transcribed onto paper tape for computer processing.
This entire procedure was tedious and error-prone. Even with two
operators, one to set the cursor and another to push the buttons
and count frames, reading a single film required several hours.

The principal requirement, then, for an improved film read-
ing system was an increase in the automation of the measurement
operation. Scanning can be done completely by machine, but the
cost would be high and the labor saved would not be as great as
one might expect. The scanning machines, which can be electro-
mechanical or completely electronic, accept the film frame by frame,
so that labor would be needed to cut the film, mount it, number the
frames, and feed them to the machine in proper order. In order to
detect the desired target on the subject in each frame, a computer
must perform pattern recognition on the raw scanner data. Such a
system was considered early in the course of this project and was
rejected because the cost per film was much higher than for any
other system.

4.3 FILM ANALYSIS TECHNIQUES

A programmable calculator* provides the basis for an inter-
mediate system, as shown in Figure 13. The projector's beam is
directed by two mirrors so that the image appears at the working
surface of the X-Y digitizer.** The digitizer's cursor contains
a cross-hair which the operator places upon a point of the image.
When the operator pushes a button on the cursor, the digitizer
electronics unit transfers the coordinates of the point to the
calculator. Two points per frame determine the slope S of a line
in the image, and the calculator computes θ = arc tan S. The
digitizer electronics can be set to sound a "beep" signal so that
the operator knows that he has taken two valid data points. The
values of θ can then be recorded in two ways: in graphic form on

---

*Hewlett-Packard Model 9100A
**Hewlett-Packard Model 9107A

17

the plotter* which attaches directly to the calculator, or in printed form (with paper tape optional) on the teletype which attaches to the coupler-controller**, which in turn is controlled by the calculator. In the near future an optional card will be added to the coupler-controller. This card will contain relays which the calculator can open and close, replacing the manual single-frame push-button of the projector. The system will then advance the film automatically when two valid data points have been taken.

The high speed cameras place timing marks on the film so that the exact frame rate may be known. If the timing marks come at a slightly higher or lower rate than the frames, the marks will appear to move relatively slowly along the edges of the frames. The number of frames needed for one complete "cycle" in this manner gives the exact frame rate. For instance, 23 timing marks (occurring at 1 mark/msec) in 22 frames imply a frame rate of $23/22 = 1.045$ msec/frame. This accuracy is needed when comparing film data to data recorded on magnetic tape.

Additional techniques must be employed to process data obtained during tests with airbags. During part of such a test, the subject's head is partly surrounded by the bag. The camera which films the action from a position directly to the side (i.e., with its lens axis perpendicular to the subject's plane of motion) then loses sight of the target and there is a gap in the angular position data which can be recovered from the film, as shown in the sample data of Figure 14. To fill in this gap, another camera is used to film the event from above and behind the subject; its position is similar to that of a passenger, in the middle of the rear sear of an automobile, who is observing the passenger in the right front seat. The film from this camera can yield angular measurements for the entire duration of the test, but these measurements must be corrected to account for the non-perpendicular direction from which the camera records the event.

---

*Hewlett-Packard Model 9125B
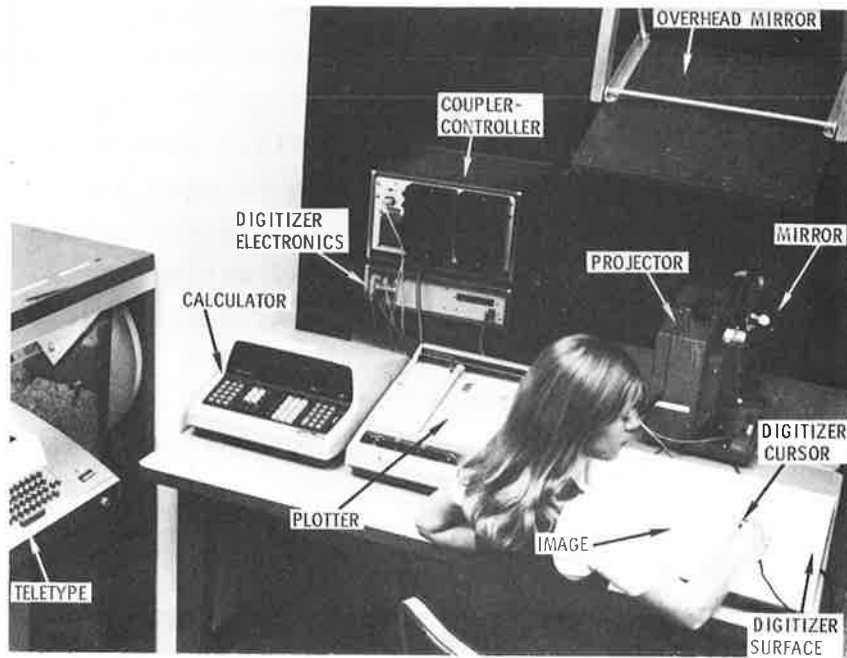**Hewlett-Packard Model 2570A
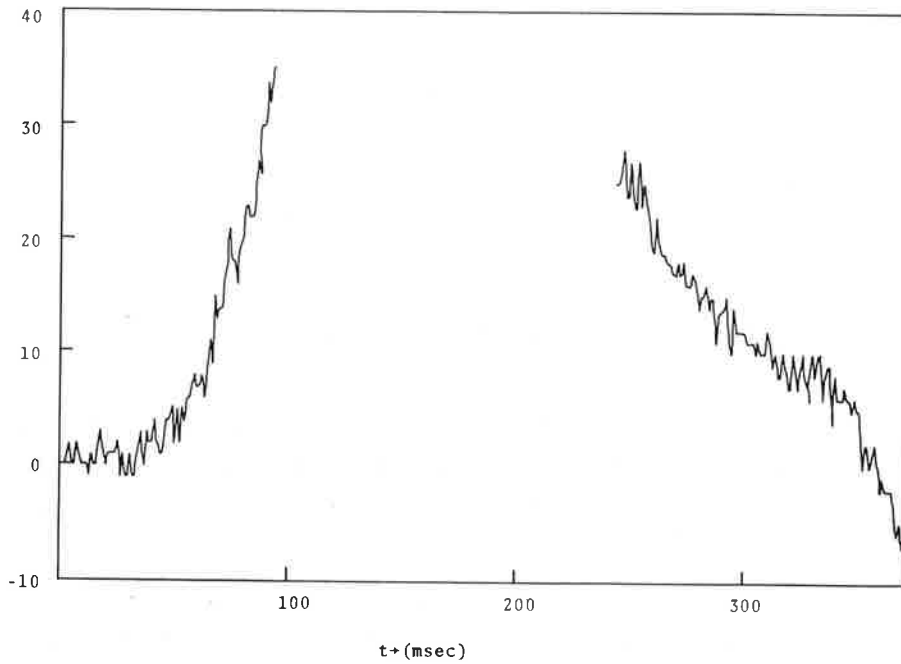
Figure 13. Calculator-Based Film Reading System

t→(msec)

Figure 14. True Angular Position (θ_T) with Perpendicular
View from Camera

19

To accomplish this we define θ_m as the angular position as measured from the film taken by the non-perpendicular camera. We wish to convert θ_m to the true value that would be measured from a perpendicular position; this true value we define as θ_T. In Figure 15 we illustrate the transformation from θ_m to θ_T. View (a) shows a night triangle as it would be seen from a perpendicular view; this triangle represents θ_T for this view, with the hypotenuse of the triangle being the relative head position and the legs X_T and Y_T filled in to illustrate the geometrical transformation caused by a change in viewing position. Let us consider the effect of elevating the camera so that it is higher than the subject's head. This can be simulated by looking at 15a and rotating the figure about the X_T axis; the result appears in 15b. The amount of change in Y_m from Y_T depends on the amount of rotation (i.e., elevation) θ_y, as shown in the figure. The effect of rotation of the camera from the perpendicular view to one from a "rear quarter" is similar, as shown in 15c. The actual position of our camera is a combination of (b) and (c), in a position which views the subject from "over the shoulder." Combining the transformation equations in (b) and (c) into one, we get:

$$\tan \theta_T = \tan \theta_m \ \frac{\cos \theta_x}{\cos \theta_y}$$

or:

$$\theta_T = \tan^{-1} \left(\tan \theta_m \ \frac{\cos \theta_x}{\cos \theta_y} \right)$$

We now wish to fill in the gap in θ_T (Figure 11) by using θ_m from the film from the non-perpendicular camera. θ_m for this test is shown in Figure 16. We must note that θ_x and θ_y do not remain constant throughout the test because of the motion of the subject away from the camera so we must compare θ_m to θ_T at several points and compute the value of $(\cos \theta_x / \cos \theta_y)$ to be used over the time interval close to each such point. To fill in the left half of the gap in θ_T, we extrapolate using the values of θ_m and θ_T closest to the left end of the gap, at t = 90 msec. Here $\theta_T = 34°$ and $\theta_m = 64°$, so:

20

$$\frac{Y_T}{X_T} = \tan \theta_T$$
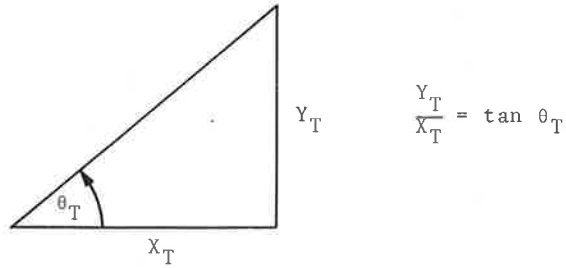
(a) Perpendicular View

$$\tan \theta_m = \frac{Y_m}{X_m} = \frac{Y_T \cos \theta_Y}{X_T} = \tan \theta_T \cos \theta_Y$$

(Since $Y_m = Y_T \cos \theta_Y$)

$Y_m < Y_T$

axis of rotation for θ_Y
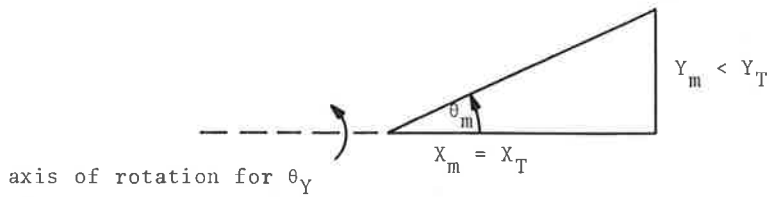
(b) Elevated View
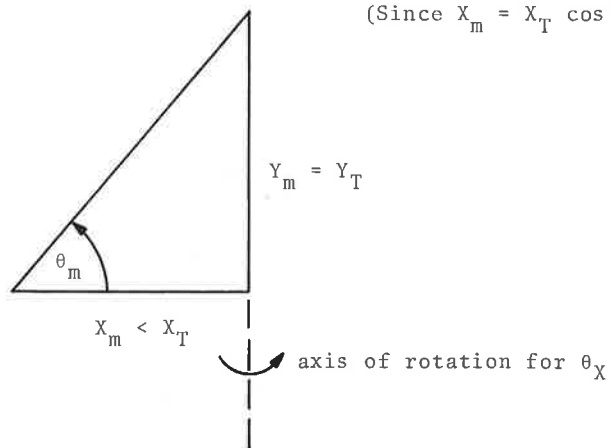
$$\tan \theta_m = \frac{Y_m}{X_m} = \frac{Y_T}{X_T \cos \theta_X} = \frac{\tan \theta_T}{\cos \theta_X}$$

(Since $X_m = X_T \cos \theta_X$)

$Y_m = Y_T$

$X_m < X_T$

axis of rotation for θ_X

(c) Rotated View

Figure 15.   Effect of Change in Camera Viewing Position
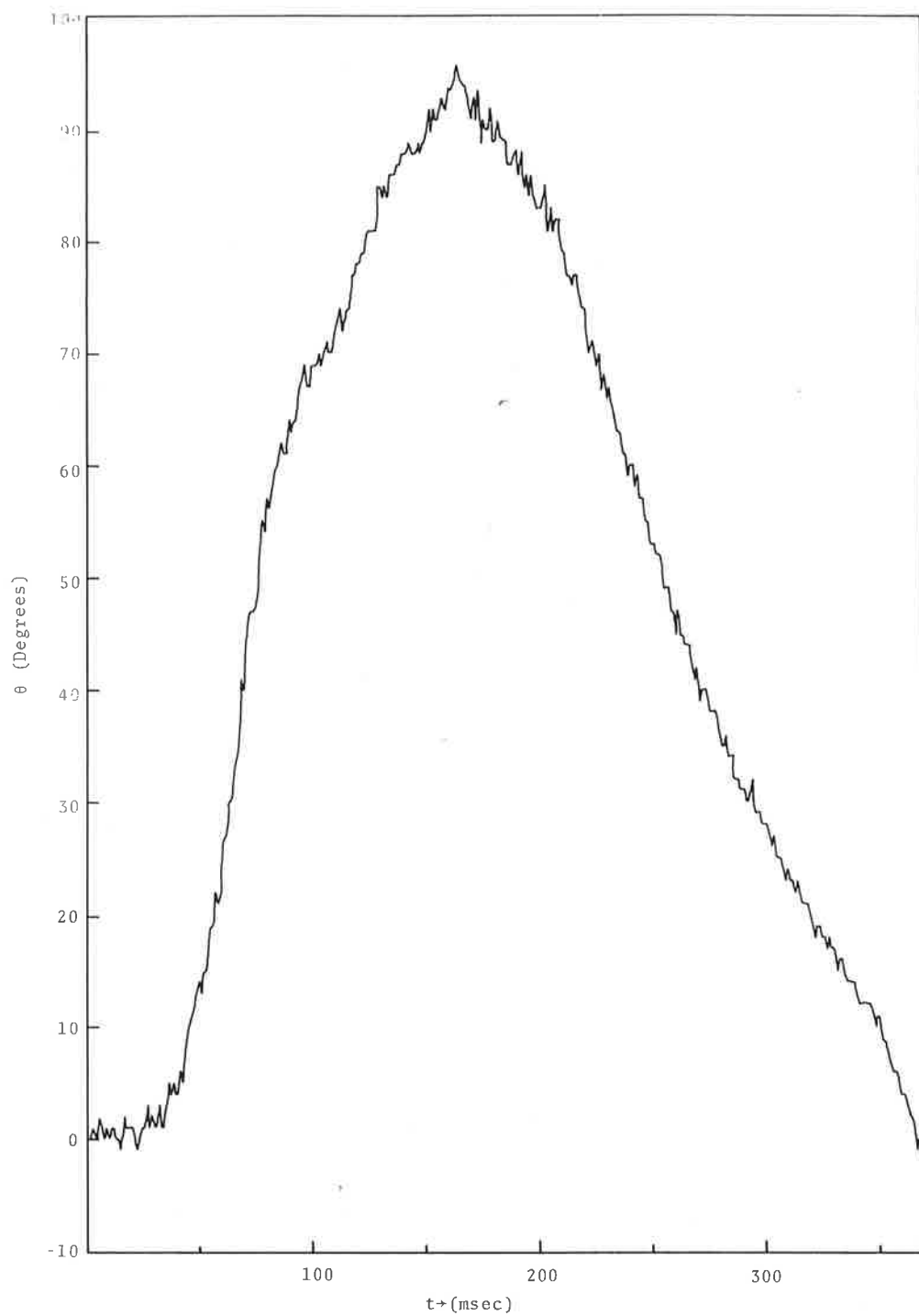
21

Figure 16. Measured Angular Position (θ_m) with Non-Perpendicular View from Camera

22

$$\frac{\cos X}{\cos Y} = \frac{\tan \theta_T}{\tan \theta_m} = \frac{\tan 34°}{\tan 64°} = .328$$

Our transformation then becomes:

$$\theta_T = \tan^{-1} \ .328 \ \tan \theta_m$$

And, for example, at t = 150 msec:

$$\theta_T = \tan^{-1} \ .328 \ \tan 89° = 87°$$

The right half of the gap in θ_T is similarly filled by referring to θ_m and θ_T at t = 250 msec. When enough points are taken to fill the gap, they can be connected with a smooth line to give a complete composite θ (Figure 17).

Figure 18 shows the final complete curve for θ for the sample film. The smooth curve is the combination of the measured θ_T (Figure 14) and the calculated θ (Figure 17) after filtering. The various corresponding events in the airbag crash test are also shown.

When filtered at 50 Hz to remove noise and differentiated to find $\dot{\theta}$, the angular velocity, the data from Figure 18 yielded the curve shown in Figure 19, which is comparable in all significant details to the curve derived by "integrating $\ddot{\theta}$" as recorded from the angular accelerometer described elsewhere in this report.

4.4 ACCURACY OF PHOTOGRAMMETRIC METHOD

Several types of noise affect the accuracy of the photogrammetric method. Principal noise sources are the following:

1. The targets on the subject's head, which were made of thin paper or cardboard, tended to bend and distort during the test. The use of stiffer targets, perhaps of thin plastic or metal, is indicated for future tests.

2. The grain of the film; this depends upon the type of film.

23

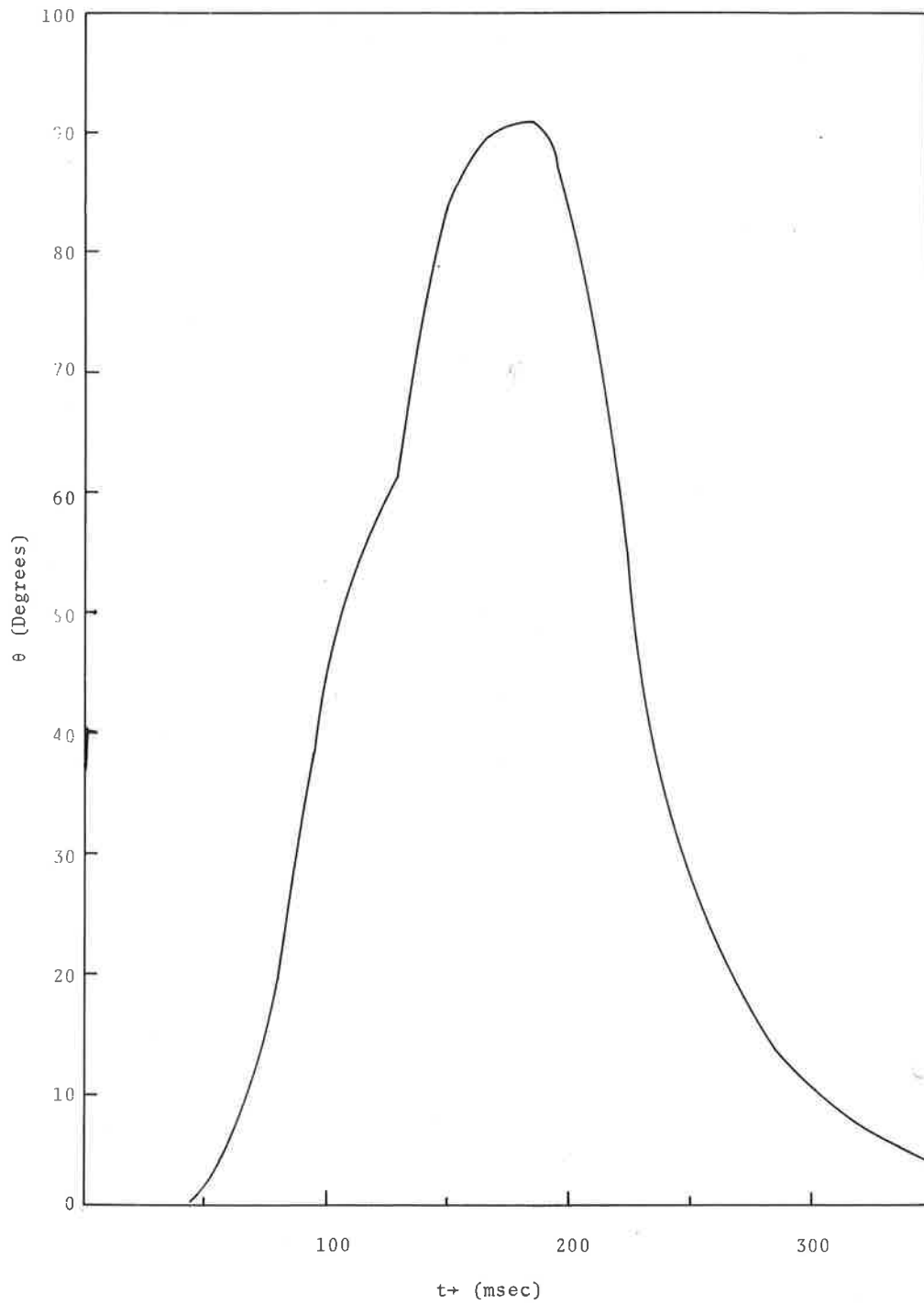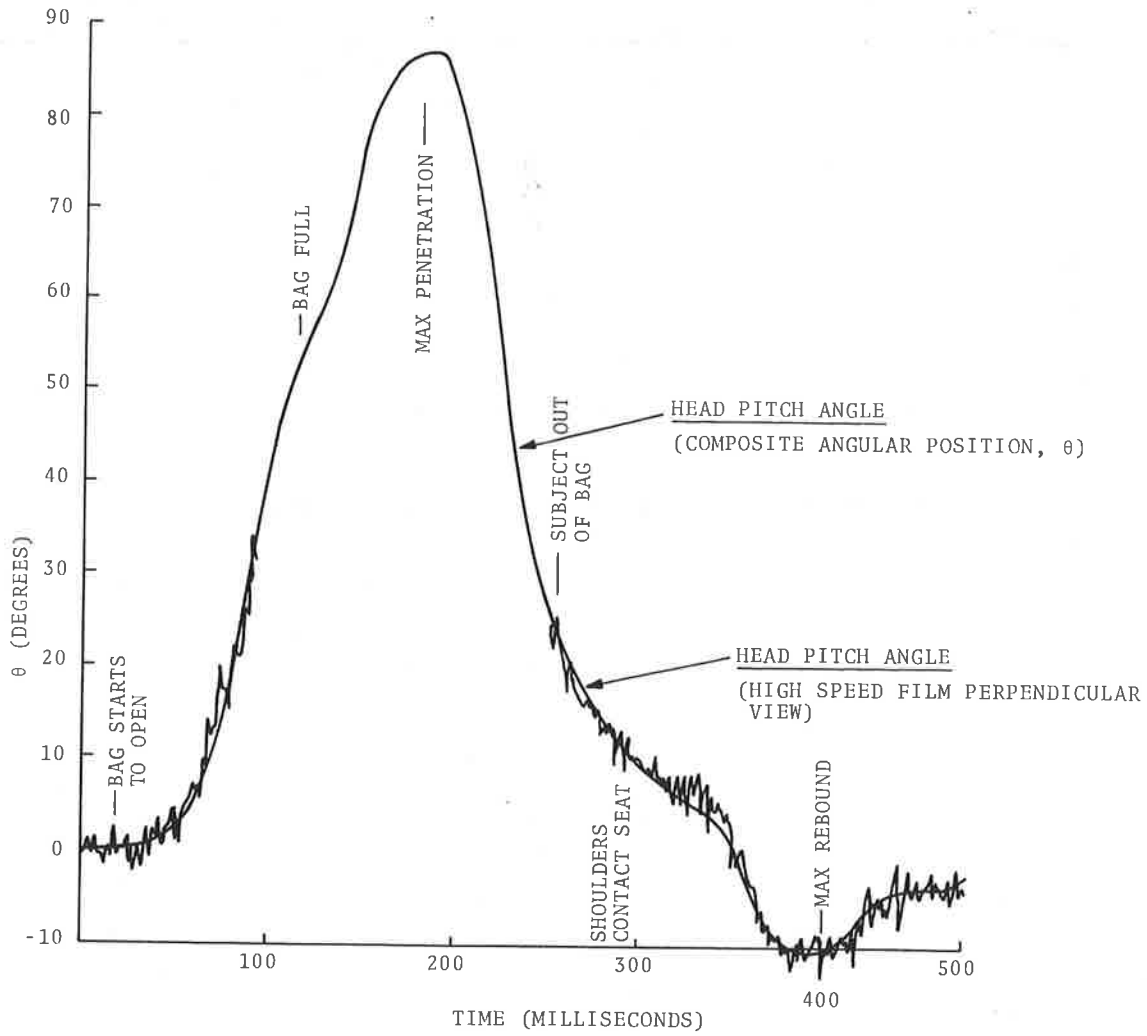Figure 17.   Composite Angular Position (θ)

Figure 18. True (θ_T) and Composite (θ) Angular Position with Events Shown
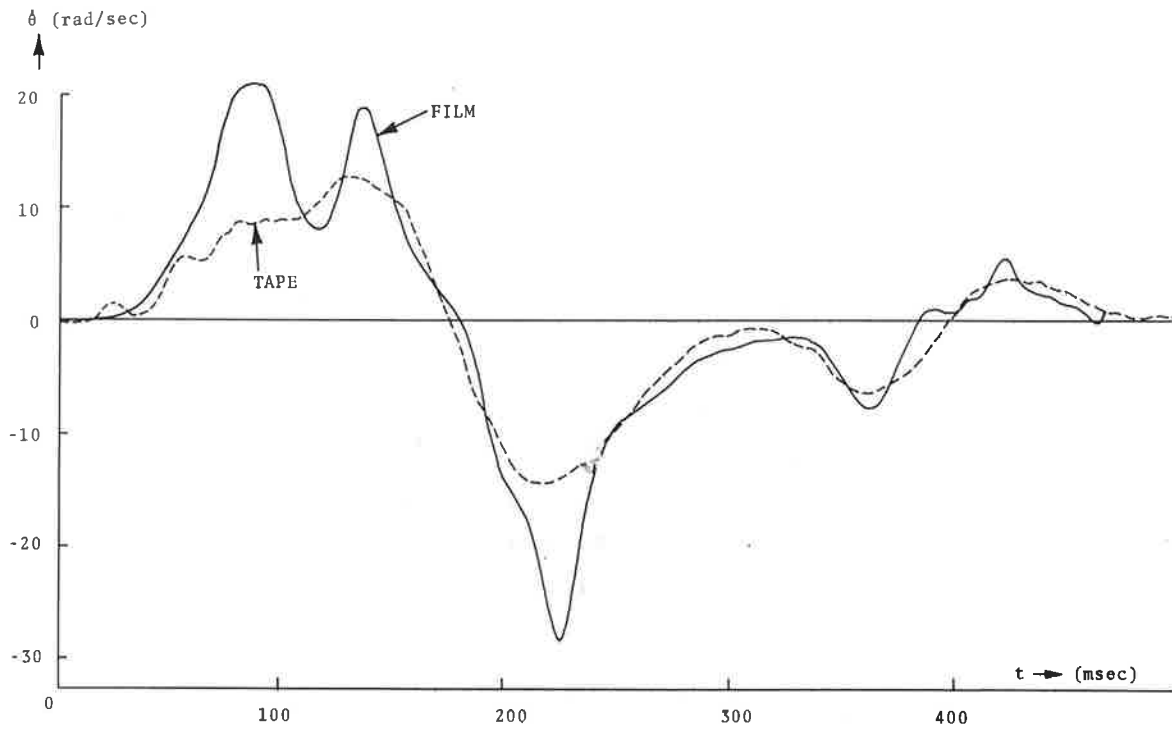
25

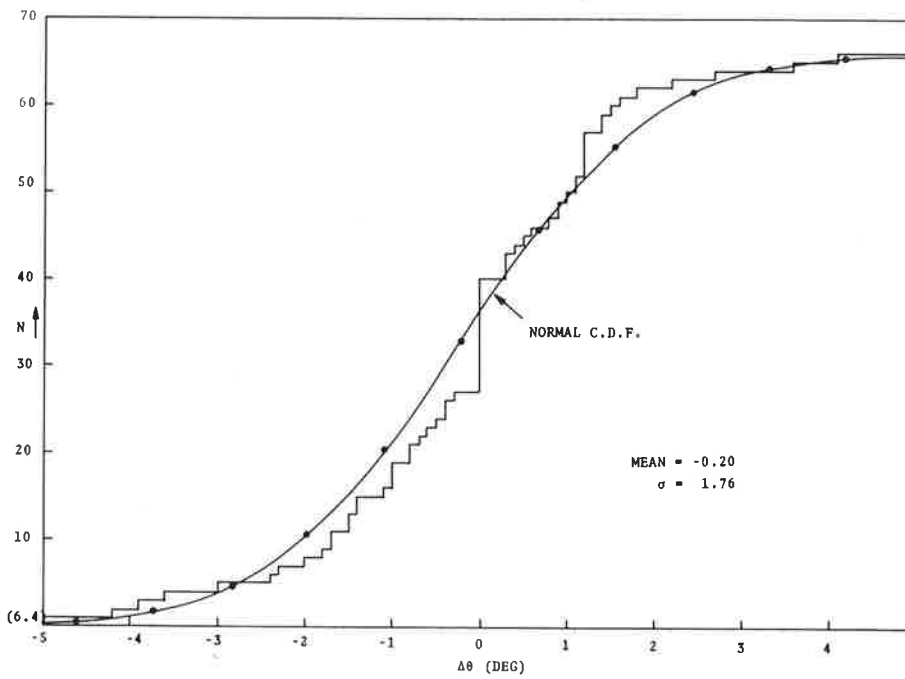Figure 19.   Comparison of Film and Tape Data

Figure 20.   Cumulative Distribution Function for Film Noise

26

3. The slight jitter in the film, which is caused by the high speed of the camera or the projector registration.

4. The poor definition in the image of the line on the target. This partly depends upon the type of film, but the lenses of the camera and projector are more important.

The relative importance of these factors is under current investigation. We can obtain a measurement of their total effect on the accuracy of the system by, first, comparing the noisy raw data measured directly from the film (Figure 14) with smooth filtered data (Figure 18) and ignoring the interval where no raw data were present. At each small grid line on the time axis, calculate $\Delta\theta$, the difference between the raw and smoothed data points. Sixty-six such values were measured and the cumulative distribution function (c.d.f) is shown in Figure 20. The c.d.f. is defined as the number of points for which $\Delta\theta$ was less than or equal to a given value. For these points, the mean was - 0.02, close to zero, as we expect for noise. The standard deviation was 1.76; the c.d.f. for a normal (Gaussian) distribution with this mean and standard deviation is also shown in Figure 20. The two curves are quite similar, so we conclude that the noise in the film-reading procedure is similar to Gaussian noise. Most of the points were within ±3°; with an overall signal range of 100°, this means that the accuracy of the process is about 3 percent.

5. COMPUTER ANALYSIS OF DATA FROM MAGNETIC TAPE

5.1 DATA REDUCTION

An analog-to-digital (A/D) converter option has been added to the Honeywell DDP-516 computer at TSC. This transfers data from a magnetic tape recorder directly into the computer. The A/D converter accepts input voltages over the range -10v to + 10v and converts it to the digital range -4096 to +4095; i.e., one digital level equals approximately 2.5 mv. This is much more accurate than any devices used to create and store the original analog signal. The maximum sampling rate is limited by the speed of the program which calls for the samples. In practice, over 20,000 samples/sec may be taken. A multiplexer allows successive samples to be taken from different input lines; the controlling program can set any order it wishes for up to 32 inputs. A sample-and-hold amplifier reduces the effective length of each sample to 0.1 μsec; the signals expected in our project change much slower that this and can be expected to remain constant over this sampling aperture.

The programs which use the A/D converter are shown in Figures 21 and 22, annotated to show the major operations. The section called "idling loop" in the main program prevents any action until the signal on a certain tape channel (here, the deceleration of the test sled) reaches a certain level; the program then proceeds because it has reached the actual data on the tape. The "read data" section uses the variables IB1, ..., IB7 to receive data from the subroutine SEVN. The rest of the main program uses a subroutine SEARCH, which is a feature of the computer's Disc Operating System*, to save the data on disc storage in seven separate files TEM 1,..., TEM 7. In the subroutine SEVN, the timing loop waits for an external signal to reach a certain level; here the signal was a signal generator with a 2KHz sine wave, thus guaranteeing 2000 samples/sec. The rest of the subroutine scans

---

*DOT-TSC-OST-72-14, May 1972

```
      COMMON IB7,IB6,IB5,IB4,IB3,IB2,IB1
      COMMON /IA/I1(1000)/IB/I2(1000)/IC/I3(1000)/ID/I4(1000)
    1 /IE/I5(1000)/IG/I6(1000)/IH/I7(1000)
2     CALL SEVN
      IF (IB7 .GE. -500) GO TO 2        ] IDLING LOOP
      DO 1 I=1,1000
      CALL SEVN
      I1(I)=IB1
      I2(I)=IB2
      I3(I)=IB3
      I4(I)=IB4                           READ DATA
      I5(I)=IB5
      I6(I)=IB6
1     I7(I)=IB7
      CALL SEARCH (2,6HITEM1  ,2)
      WRITE (4,10) I1
      CALL SEARCH (4,0,2)
      CALL SEARCH (2,6HITEM2  ,2)
      WRITE (4,10) I2
      CALL SEARCH (4,0,2)
      CALL SEARCH (2,6HITEM3  ,2)
      WRITE (4,10) I3
      CALL SEARCH (4,0,2)
      CALL SEARCH (2,6HITEM4  ,2)
      WRITE (4,10) I4
      CALL SEARCH (4,0,2)                 STORE DATA ON TAPE
      CALL SEARCH (2,6HITEM5  ,2)
      WRITE (4,10) I5
      CALL SEARCH (4,0,2)
      CALL SEARCH (2,6HITEM6  ,2)
      WRITE (4,10) I6
      CALL SEARCH (4,0,2)
      CALL SEARCH (2,6HITEM7  ,2)
      WRITE (4,10) I7
      CALL SEARCH (4,0,2)
10    FORMAT ((10I7))
      CALL SEARCH (4,0,2)
      CALL EXIT
      END
$0
```

Figure 21. Main Tape-Reading Program

```
        SUBR    SEVN
        REL
SEVN    DAC     **
LOOP    LDA     =0      ⎫
        OTA     '1423   ⎪
        JMP     *-1     ⎪
        INA     '1233   ⎬  TIMING LOOP
        JMP     *-1     ⎪
        CAS     =3000   ⎪
        JMP     LOOP    ⎭
        NOP
        LDA     =1      ⎫
        OTA     '1423   ⎪
        JMP     *-1     ⎪
        INA     '1233   ⎬  IB1
        JMP     *-1     ⎪
        STA     '63776  ⎭
        LDA     =2      ⎫
        OTA     '1423   ⎪
        JMP     *-1     ⎪
        INA     '1233   ⎬  IB2
        JMP     *-1     ⎪
        STA     '63775  ⎭
        LDA     =3      ⎫
        OTA     '1423   ⎪
        JMP     *-1     ⎪
        INA     '1233   ⎬  IB3
        JMP     *-1     ⎪
        STA     '63774  ⎭
        LDA     =4      ⎫
        OTA     '1423   ⎪
        JMP     *-1     ⎪
        INA     '1233   ⎬  IB4
        JMP     *-1     ⎪
        STA     '63773  ⎭
        LDA     =5      ⎫
        OTA     '1423   ⎪
        JMP     *-1     ⎪
        INA     '1233   ⎬  IB5
        JMP     *-1     ⎪
        STA     '63772  ⎭
        LDA     =6      ⎫
        OTA     '1423   ⎪
        JMP     *-1     ⎪
        INA     '1233   ⎬  IB6
        JMP     *-1     ⎪
        STA     '63771  ⎭
        LDA     =7      ⎫
        OTA     '1423   ⎪
        JMP     *-1     ⎪
        INA     '1233   ⎬  IB7
        JMP     *-1     ⎪
        STA     '63770  ⎭
        JMP*    SEVN
        END
$0
```

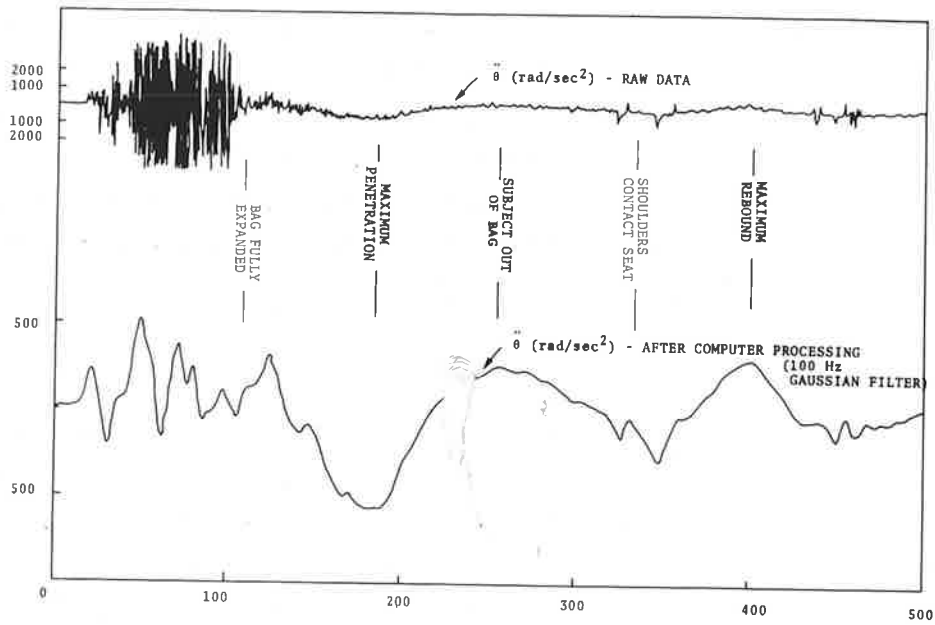Figure 22.   Tape-Reading Subroutine

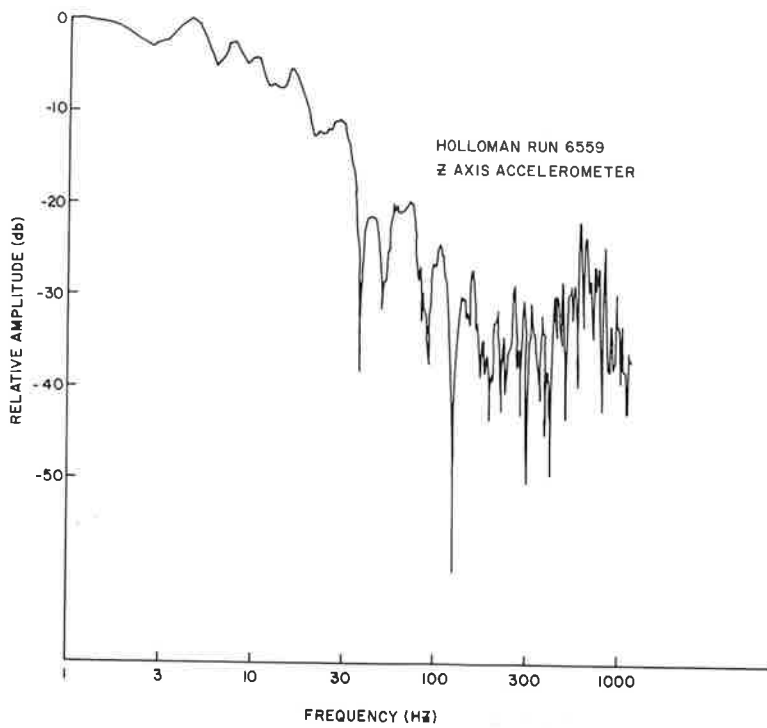Figure 23.   Example of Signal Processing by Computer

Figure 24.   Fourier Spectrum

seven input lines in order and stores the data in IB1,..., IB7.

The contents of one of the files described above for one data run are shown in the upper curve of Figure 23. This signal needed to be scaled and filtered; this was done using a program which included the Fast Fourier Transform*. The result is shown in the lower curve in Figure 24. This curve, when integrated numerically on the computer, gave the value for $\dot{\theta}$ marked "TAPE" on Figure 19 in the preceding section.

5.2 FOURIER SPECTRUM

Due to the continuing concern about the information bandwidth present in measurements of head accelerations, a frequency analysis was performed on one of the data channels. The result of this analysis is shown in Figure 24. The result is quite similar to that found previously,** in that there seems to be little information above 100 Hz.

---

*DOT-TSC-NHTSA-71-4, July 1971

**DOT-HS-820-211

32

6. SUMMARY

A piezoresistive mouthpiece accelerometer has been developed for use during crash tests. The accelerometer is capable of measuring three orthogonal linear accelerations and the rotational acceleration in the sagittal plane of a subject's head. The device has been successfully tested in the laboratory on a shake table and in the field on both humans and dummies. The noise previously encountered with piezoelectric accelerometers has been reduced through the use of piezoresistive devices. The linear sensitivity of the rotational accelerometer has been reduced to a level of 3.3 rad/sec^2/g.

Film analysis has been semi-automated by utilizing a programmable calculator, x-y digitizer and a plotter. The reduction of high speed film data is now a relatively easy proceedure. The differentiation of the positional information derived from high speed films is in agreement with the integration of the information obtained from the accelerometers.

In order to further reduce the noise artifacts in the system, the use of voltage controlled oscillators (generating subcarriers) placed in the signal path near the accelerometer package is being investigated. The use of an RF telemetry link is being considered in order to eliminate acoustical noise picked up by the signal cables from the test sled.